SCINDEKS
Serbian Citation Index
J Med Biochem 2026; 45 DOI: 10.5937/jomb0-66487

UDK 577.1 : 61 **ISSN 1452-8258**

J Med Biochem 45: 1–11, 2026

Original paper
Originalni naučni rad

DIFFERENTIAL EXPRESSION OF PREOPERATIVE CHOLESTATIC BIOCHEMICAL PROFILES, INFLAMMATORY FACTORS, AND ELECTROLYTES: RISK STRATIFICATION BASED ON COMPLICATED GS

DIFERENCIJALNA EKSPRESIJA PREOPERATIVNIH HOLESTATSKIH BIOHEMIJSKIH PROFILA, INFLAMATORNIH FAKTORA I ELEKTROLITA: STRATIFIKACIJA RIZIKA ZASNOVANA NA KOMPLIKOVANOJ KOLELITIJAZI

Xuecui Ge[1#], Tingting Zhang[1#], Changzhou Zhang[1], Dalu Liu[1], Chun Zhang[1]*

[1]Department of General Surgery, the First People's Hospital of Chuzhou Affiliated to Anhui Medical University, Chuzhou, Anhui, 239000, China

Summary

Background: Gallstones (GS) are a highly prevalent digestive disorder worldwide and can readily progress to complicated GS. Most previous studies on GS have focused on isolated indicators. At the same time, the interplay among multisystem biochemical markers has received far less attention; the mechanisms underlying this interplay in disease progression remain poorly understood. The present study was designed to systematically compare preoperative multidimensional biochemical indices between patients with simple GS and those with complicated GS, and to provide laboratory evidence for clarifying the mechanisms underlying disease progression.
Methods: A total of 107 preoperative patients with GS confirmed by imaging between January 1, 2024 and December 31, 2025, were included, including 49 patients in the simple GS group and 58 in the complicated GS group. The test panel covered five modules: the core cholestatic biochemical profile (10 items), bile duct-specific injury and metabolic regulatory markers (GST-α, C4, and FGF19), inflammation- and tissue remodelling-related markers (10 items), electrolyte and acid-base homeostasis indices (10 items), and 15 bile acid subspecies.
Results: The core cholestatic indices were significantly elevated in the complicated group, with TBIL and GGT increasing by 1.87-fold and 4.82-fold, respectively (both $P<0.05$). GST-α, a bile duct-specific injury marker, was markedly upregulated, whereas the bile acid metabolic

Kratak sadržaj

Uvod: Kolelitijaza (GS) je veoma rasprostranjen poremećaj digestivnog trakta širom sveta i može da lako napreduje u komplikovani oblik. Većina dosadašnjih istraživanja se fokusirala na pojedinačne pokazatelje, dok je međusobna povezanost višesistemskih biohemijskih markera znatno manje proučavana; mehanizmi koji su u osnovi ove interakcije tokom progresije bolesti i dalje nisu dovoljno razjašnjeni. Cilj ove studije bio je da se sistematski uporede preoperativni višedimenzionalni biohemijski parametri između pacijenata sa nekomplikovanom i komplikovanom kolelitijazom, kao i da se pruže laboratorijski dokazi za razjašnjenje mehanizama progresije bolesti.
Metode: U studiju je uključeno ukupno 107 preoperativnih pacijenata sa kolelitijazom potvrđenom radiološkim metodama u periodu od 1. januara 2024. do 31. decembra 2025. godine, od čega je 49 pacijenata bilo u grupi sa nekomplikovanom, a 58 u grupi sa komplikovanom kolelitijazom. Ispitivani panel je obuhvatio pet modula: osnovni holestatski biohemijski profil (10 parametara), markere oštećenja žučnih puteva i regulacije metabolizma (GST-α, C4 i FGF19), markere povezane sa inflamacijom i remodelovanjem tkiva (10 parametara), pokazatelje elektrolitnog i acido-baznog statusa (10 parametara) i 15 podvrsta žučnih kiselina.
Rezultati: Osnovni holestatski parametri su bili značajno povišeni u grupi sa komplikovanom kolelitijazom, pri čemu su ukupni bilirubin (TBIL) i gama-glutamil transferaza (GGT)

Address for correspondence:
Chun Zhang
e-mail: zhangchun5062@outlook.com

regulators FGF19 and C4 were both downregulated (both P<0.05). Among the inflammatory markers, CRP, Presepsin, and several related indices were several-fold higher in the complicated group. These patients also showed statistically significant electrolyte alterations, including lower serum potassium and sodium levels, with a subset developing clinically significant hypokalaemia and hyponatremia, along with compensated metabolic acidosis (BE=-3.36±1.81 mmol/L). All 15 serum bile acid subspecies were significantly increased. The rise in conjugated bile acids (8- to 10-fold) was far greater than that in unconjugated bile acids (2- to 5-fold) (all P<0.05).
Conclusion: Simple and complicated GS differed significantly across multiple biochemical dimensions. The findings suggest that cholestasis, inflammatory activation, disturbance of internal homeostasis, and abnormal bile acid metabolism act in concert and form a vicious cycle during the transition from simple to complicated GS.

Keywords: gallstones, cholestasis, bile acid profiling, inflammatory markers, electrolyte imbalance, biomarkers

porasli 1,87 puta, odnosno 4,82 puta (oba P<0,05). GST-α, marker specifičan za oštećenje žučnih puteva je bio značajno povišen dok su regulatori metabolizma žučnih kiselina FGF19 i C4 bili sniženi (oba P<0,05). Među inflamatornim markerima, CRP, presepsin i više povezanih pokazatelja bili su višestruko viši u komplikovanoj grupi. Kod ovih pacijenata zabeležene su i statistički značajne promene elektrolita, uključujući niže koncentracije kalijuma i natrijuma u serumu, pri čemu je kod jednog dela ispitanika razvijena klinički značajna hipokalemija i hiponatremija, uz kompenzovanu metaboličku acidozu (BE=-3,36±1,81 mmol/L). Svih 15 podvrsta žučnih kiselina u serumu je bilo značajno povišeno. Porast konjugovanih žučnih kiselina (8–10 puta) je bio znatno izraženiji nego porast nekonjugovanih (2–5 puta) (sve P<0,05).
Zaključak: Postoje značajne razlike između nekomplikovane i komplikovane kolelitijaze u više biohemijskih dimenzija. Nalazi ukazuju da holestaza, inflamatorna aktivacija, poremećaj unutrašnje homeostaze i abnormalan metabolizam žučnih kiselina deluju udruženo i formiraju začarani krug tokom prelaska iz nekomplikovanog u komplikovani oblik bolesti.

Ključne reči: kolelitijaza, holestaza, profilisanje žučnih kiselina, inflamatorni markeri, elektrolitni disbalans, biomarkeri

Introduction

Gallstones (GS) are a common benign digestive disease worldwide, with an overall prevalence of 10%–20% in adults. Of these patients, 25%–30% may progress to complicated GS, including severe phenotypes such as acute suppurative cholecystitis, bile duct obstruction, and biliary pancreatitis (1). Compared with simple GS, patients with complicated disease have a perioperative complication rate of 18%–28% and a 3- to 6-fold higher mortality rate (2). This not only adds substantially to the medical burden but also raises the bar for clarifying disease mechanisms and identifying clinically useful biochemical markers (3, 4). Cholestasis is the key initiating event in the occurrence and progression of GS. Persistent impairment of biliary excretion can damage biliary epithelial cells, thereby activating innate immunity and inflammatory cascades (5). Once the inflammatory response becomes dysregulated, biliary epithelial injury and bile excretory dysfunction worsen further. At the same time, inflammatory stress and biliary obstruction can disrupt electrolyte and acid-base homeostasis, forming a vicious cycle that drives the transition from simple to complicated disease (6).

Most laboratory studies of GS have centred on routine liver function tests and inflammatory markers examined in isolation (2, 7). In contrast, biliary epithelial injury markers, bile acid subspecies, inflammation-derived indices, and acid-base variables have received much less attention. Although previous studies have shown that some cholestasis-related biochemical markers and inflammatory mediators are abnormally expressed in patients with GS, the internal links and coordinated changes among these multidimensional indices remain insufficiently defined (8). Nor has the laboratory profile that distinguishes simple from complicated GS been fully delineated. At present, systematic observational studies are still lacking that simultaneously cover the core cholestatic biochemical profile, bile duct-specific injury and metabolic regulatory markers, inflammation- and tissue remodelling-related indicators, electrolyte and acid-base homeostasis, and bile acid subspecies. As a result, a coherent laboratory framework for understanding the pathophysiology of GS progression is still lacking.

Against this background, the present study enrolled patients with GS and systematically compared the preoperative expression of multidimensional laboratory indices between simple and complicated disease. We systematically compared the expression differences of multidimensional biochemical indices between the two groups. We analysed their coordinated changes during disease progression. These findings provide a clearer picture of the biochemical changes that accompany GS progression, offer new experimental evidence for understanding its pathophysiological basis, and provide a useful reference for subsequent work in clinical biochemistry.

Materials and Methods

Study design

This was a single-centre retrospective observational study. Patients with GS diagnosed by abdominal imaging in our institution between January 1, 2024, and December 31, 2025, were consecutively enrolled. All data collection was completed by December 31, 2025, consistent with the retrospective study design. The study protocol was reviewed and approved by the institutional ethics committee. All procedures were conducted in accordance with the ethical principles of the Declaration of Helsinki, and the institutional ethics committee approved the waiver of written informed consent due to the study's retrospective nature. *Figure 1* illustrates the main flow of this study.

Study population

According to imaging findings and pathological classification, the study population was divided into a simple GS group (n=49) and a complicated GS group (n=58). The inclusion criteria were as follows: ① GS confirmed by abdominal ultrasonography, CT, or MRI; ② completion of the full panel of laboratory tests within 72 h before surgery, with complete specimens and data available; and ③ complete demographic baseline information. The exclusion criteria were as follows: ① hepatobiliary diseases that could interfere with bile metabolism, inflammatory status, or electrolyte homeostasis, including hepatobiliary malignancies, cirrhosis, active chronic viral hepatitis, and primary biliary cholangitis; ② treatment within 1 month before enrolment with anti-infective agents, glucocorticoids, immunomodulators, or other drugs that might affect biochemical or inflammatory measurements; ③ systemic diseases that could interfere with laboratory testing, including autoimmune diseases, moderate to severe anaemia (haemoglobin <90 g/L), coagulation disorders (INR >1.5 or APTT prolonged >10 s), major organ failure, and systemic malignancies; ④ pregnancy or lactation; and ⑤ specimens affected by haemolysis, lipemia, or other analytical interference, or missing core laboratory data. Simple GS was defined as gallstones confirmed by imaging without complications such as acute cholecystitis, bile duct obstruction, biliary pancreatitis, gallbladder perforation, or gangrene; complicated GS was defined as the presence of at least one of these complications.

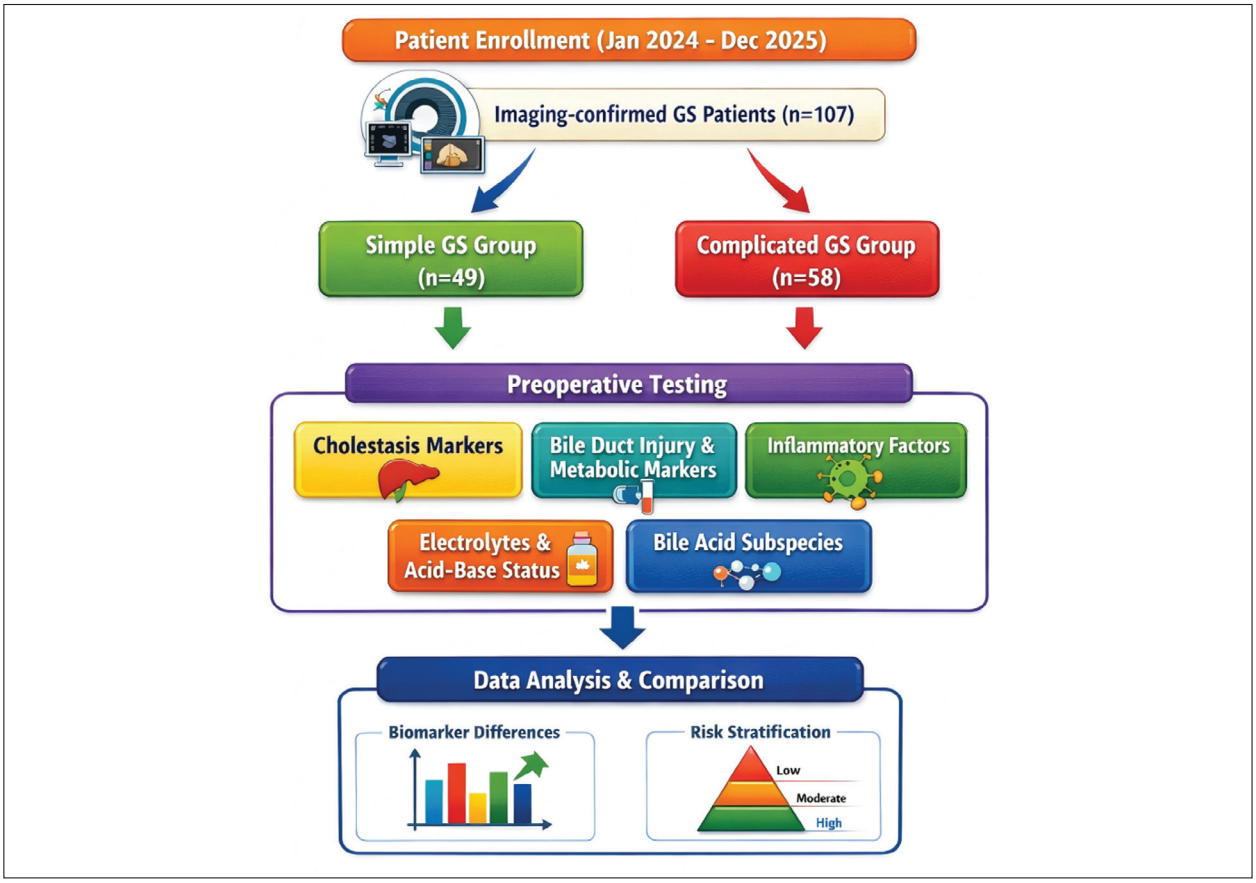

Figure 1 The main flow of this study.

Sample collection and processing

Fasting peripheral venous blood was collected from each participant in the early morning, within 72 h before surgery. Corresponding specimens were obtained using BD Vacutainer additive-free clot activator tubes, EDTA-K_2 anticoagulant tubes, and lithium heparin anticoagulant tubes (BD, USA). After collection, all samples were immediately sealed, protected from light, and transported. Serum and plasma were separated by centrifugation at 3000×g for 15 min at 4 °C. The supernatant was aliquoted into 200 µL per tube and stored immediately in a -80 °C ultra-low-temperature freezer, protected from light, until batch analysis to avoid repeated freeze-thaw cycles.

Laboratory testing

Certified laboratory technicians performed all assays in strict accordance with standardized clinical laboratory procedures. Internal quality control (IQC) and external quality assessment (EQA) were implemented throughout. For all analytes, the maximum acceptable intra-assay coefficient of variation (CV) was <5%, and the inter-assay CV was <8%. The actual CVs for individual assays were lower, as detailed in the respective method sections.

Determination of the core cholestatic biochemical profile

The panel included Total Bilirubin (TBIL), Direct Bilirubin (DBIL), Indirect Bilirubin (IBIL), γ-Glutamyl Transpeptidase (GGT), Alkaline Phosphatase (ALP), Total Bile Acid (TBA), Alanine Aminotransferase (ALT), Aspartate Aminotransferase (AST), 5′-Nucleotidase (5′-NT), and Leucine Aminopeptidase (LAP). All measurements were performed on a Hitachi 7600 fully automated biochemical analyser (Hitachi High-Tech Corporation, Japan), and all reagents, calibrators, and high- and low-level quality control materials were supplied by the original manufacturer. During testing, the reaction temperature was maintained at 37 °C, and the cuvette optical path length was 1 cm. The detection wavelength for each analyte was set strictly according to the reagent instructions. One set of high- and low-level quality control materials was inserted after every 20 specimens to monitor system stability. In the end, the intra-assay CVs for all indices were <3.5%, and the inter-assay CVs were <6%. The linear ranges for key cholestatic analytes were as follows: TBIL, 0.5–513 µmol/L; GGT, 3–1200 U/L.

Assays for bile duct-specific injury and metabolic regulatory markers

Glutathione S-transferase α (GST-α) was quantified by enzyme-linked immunosorbent assay (ELISA) using a kit from R&D Systems, USA (catalogue No. DGSTA0). All procedures were carried out strictly according to the manufacturer's instructions. Absorbance was read on a Molecular Devices SpectraMax i3x microplate reader (Molecular Devices, USA) at 450 nm with a reference wavelength of 630 nm. 7α-Hydroxy-4-cholesten-3-one (C4) was quantified by high-performance liquid chromatography-tandem mass spectrometry (HPLC-MS/MS) using [2H7]-C4 (100 ng/mL) as the isotope-labelled internal standard. The analytical platform consisted of an Agilent 1290 Infinity II HPLC system coupled to an AB Sciex Triple Quad 4500 triple quadrupole mass spectrometer (Agilent Technologies, USA; AB Sciex, USA), and chromatographic separation was performed on an Agilent ZORBAX SB-C18 column (2.1 mm×100 mm, 3.5 µm). The elution program was as follows: 0–2 min, 30% B; 2–8 min, 30%–95% B; 8–10 min, 95% B; 10–10.1 min, 95%–30% B; and 10.1–12 min, 30% B. Fibroblast growth factor 19 (FGF19) was measured using a double-antibody sandwich electrochemiluminescence assay on a Roche Cobas e602 automated chemiluminescence immunoassay analyser (Roche Diagnostics, Germany). Matching reagents, calibrators, and quality control materials were all original manufacturer products. The reaction temperature was maintained at 37 °C, the linear range was 10–3000 pg/mL, the intra-assay CV was <4%, and the inter-assay CV was <6%.

Determination of inflammation- and tissue remodelling-related markers

Routine inflammatory markers, including C-reactive protein (CRP), procalcitonin (PCT), interleukin-6 (IL-6), tumour necrosis factor-α (TNF-α), and soluble CD14 subtype (Presepsin), were all measured on the above-mentioned Roche Cobas e602 chemiluminescence immunoassay analyser using original manufacturer reagents.

Routine hematologic parameters were measured using a Sysmex XN-9000 automated haematology analyser (Sysmex Corporation, Japan) with original manufacturer reagents and quality control materials, and cell counting was performed based on sheath-flow impedance combined with flow cytometry. Neutrophil/lymphocyte ratio (NLR) and platelet/lymphocyte ratio (PLR) were calculated. The testing environment was maintained at 22–25 °C, and internal quality control was performed twice daily to ensure system stability.

Myeloperoxidase (MPO), matrix metalloproteinase-9 (MMP-9), and tissue inhibitor of metallo-

proteinase-1 (TIMP-1) were quantified by ELISA using the methods described above, and all kits were purchased from R&D Systems, USA. The linear range of CRP was 0.3–350 mg/L.

Determination of electrolyte and acid-base homeostasis indicators

The electrolyte panel included serum potassium (K^+), sodium (Na^+), chloride (Cl^-), total calcium (Ca^{2+}), ionized calcium (iCa^{2+}), magnesium (Mg^{2+}), and phosphorus (P). Acid-base homeostasis indices included whole-blood pH, Standard Bicarbonate (SBC), and Base Excess (BE). All measurements were performed using a Radiometer ABL90 FLEX blood gas and electrolyte analyser (Radiometer, Denmark) with the manufacturer's original reagents, calibrators, and quality control materials. Quantification was based on the ion-selective electrode method. The detection temperature was maintained at 37 °C. Two-point calibration was performed before each batch, and the electrode slope range was controlled at 95%–105%. Intra-assay and inter-assay CVs for all indices were <2% and <4%, respectively.

Quantitative analysis of bile acid subspecies

Absolute quantification of bile acid subspecies was performed by HPLC-MS/MS using [2H4]-cholic acid (50 ng/mL) and [2H4]-chenodeoxycholic acid (50 ng/mL) as mixed isotope internal standards, covering five unconjugated bile acids [Cholic acid (CA), Chenodeoxycholic acid (CDCA), Deoxycholic acid (DCA), Lithocholic acid (LCA), and Ursodeoxycholic acid (UDCA)] and 10 conjugated bile acids [Glycocholic acid (GCA), Taurocholic acid (TCA), Glycochenodeoxycholic acid (GCDCA), Taurochenodeoxycholic acid (TCDCA), Glycodeoxycholic acid (GDCA), Taurodeoxycholic acid (TDCA), Glycolithocholic acid (GLCA), Taurolithocholic acid (TLCA), Glycoursodeoxycholic acid (GUDCA), and Tauro Ursodeoxycholic acid (TUDCA)]. The elution program was as follows: 0–1 min, 20% B; 1–12 min, a linear increase from 20% B to 80% B; 12–15 min, 80% B to 100% B; 15–17 min, 100% B maintained; 17–17.1 min, 100% B returned to 20% B; and 17.1–20 min, system equilibration at 20% B.

Statistical analysis

All statistical analyses were performed using SPSS 26.0 software. Quantitative data were first tested for normality using the Shapiro-Wilk test, with $\alpha=0.05$. Data conforming to a normal distribution are expressed as mean ± standard deviation, and between-group comparisons were performed using the independent-samples t-test. Data not conforming to a normal distribution are expressed as median (25th, 75th interquartile range), and between-group comparisons were performed using the Mann-Whitney U test. Categorical data are expressed as the number of cases (percentage), and between-group comparisons were performed using the χ^2 test. All statistical tests were two-sided, and $P<0.05$ was considered statistically significant.

Results

Baseline characteristics of the study population

There were no statistically significant differences between the simple and complicated groups in baseline variables such as age and sex ($P>0.05$), indicating balanced baseline characteristics and good comparability between groups (*Table I*).

Differences in expression of the core cholestatic biochemical profile

Compared with the simple GS group, the complicated group showed overall abnormalities in the core cholestatic biochemical profile, with

Table I Baseline characteristics of patients with simple and complicated GS.

Projects	Simple group (n=49)	Complicated group (n=58)	t/χ^2	P
Age (years)	51.61±9.18	54.84±11.80	1.56	0.122
Gender (male/female)	18/31	26/32	0.72	0.397
BMI (kg/m^2)	25.00±2.82	26.04±3.10	1.81	0.073
Duration of disease (years)	2.94±1.07	3.31±0.96	1.90	0.061
Combined hypertension	11 (22.45)	16 (27.59)	0.37	0.542
Combined diabetes mellitus	6 (12.24)	10 (17.24)	0.52	0.470
Combined coronary heart disease	4 (8.16)	6 (10.34)	0.15	0.699

Note: Body Mass Index (BMI)

Table II Comparison of the core cholestatic biochemical profile between the simple GS and complicated GS groups.

Indicators	unit	Simple group (n=49)	Complicated group (n=58)	t/U	P
TBIL	μmol/L	15.00 (12.57, 17.70)	28.10 (20.64, 33.74)	305.51	0.001
DBIL	μmol/L	8.44 (7.12, 9.24)	17.20 (13.04, 26.39)	244	<0.001
IBIL	μmol/L	9.11 (8.43, 9.87)	13.67 (10.67, 15.57)	415.5	<0.001
GGT	U/L	36.63 (32.14, 46.71)	176.72 (145.28, 218.21)	29	<0.001
ALP	U/L	74.59±13.92	161.69±43.32	13.49	<0.001
TBA	mmol/L	9.20 (7.71, 9.94)	23.73 (19.59, 26.78)	59	<0.001
ALT	U/L	34.04 (22.81, 44.15)	45.76 (36.25, 58.45)	793	<0.001
AST	U/L	26.81 (17.58, 35.82)	40.53 (31.70, 55.16)	729	<0.001
5′-NT	U/L	4.90±1.10	12.34±3.27	15.21	<0.001
LAP	U/L	32.67±7.49	64.13±12.19	15.72	<0.001

Note: Data are presented as mean ± standard deviation for normally distributed variables (analysed by independent-samples t-test) and median (25th, 75th interquartile range) for non-normally distributed variables (analysed by Mann-Whitney U test). Total Bilirubin (TBIL), Direct Bilirubin (DBIL), Indirect Bilirubin (IBIL), γ-Glutamyl Transpeptidase (GGT), Alkaline Phosphatase (ALP), Total Bile Acid (TBA), Alanine Aminotransferase (ALT), Aspartate Aminotransferase (AST), 5′-Nucleotidase (5′-NT), Leucine Aminopeptidase (LAP)

Table III Comparison of bile duct-specific injury and metabolic regulatory markers between the simple GS and complicated GS groups.

Indicators	unit	Simple group (n=49)	Complicated group (n=58)	t/U	P
GST-α	ng/mL	2.62 (1.91, 3.40)	10.12 (7.90, 12.85)	45	<0.001
C4	ng/mL	45.48±11.59	21.91±9.45	11.57	<0.001
FGF19	pg/mL	137.08±46.73	76.17±22.79	8.77	<0.001

Note: Glutathione S-transferase a (GST-a), 7a-Hydroxy-4-cholesten-3-one (C4), Fibroblast growth factor 19 (FGF19)

changes consistent with the pathophysiological pattern of obstructive jaundice. More specifically, median TBIL in the complicated group was 28.10 μmol/L, 1.87 times that observed in the simple group (15.00 μmol/L; P=0.001). Median DBIL was 17.20 μmol/L, representing a 103.79% increase over the 8.44 μmol/L recorded in the simple group (P<0.001), which is consistent with the bilirubin pattern typically seen in biliary obstruction. Among bile duct-specific enzymatic markers, median GGT reached 176.72 U/L, 4.82 times that of the simple group (P<0.001). ALP, 5′-NT, and LAP also rose markedly in parallel (P<0.001). At the same time, ALT and AST, which reflect secondary hepatocellular injury, were likewise higher in the complicated group (P<0.001).

Differences in expression of bile duct-specific injury and metabolic regulatory markers

Among the three targeted markers measured in this study, GST-α, a bile duct epithelial cell-specific injury marker, was markedly upregulated in the complicated group, with a median value of 10.12 ng/mL, representing a 386.26% increase over the simple group (P<0.001). This closely reflected the degree of biliary epithelial injury in patients with complicated GS. By contrast, both key markers along the bile acid regulatory axis were reduced, with C4 falling to 21.91±9.45 ng/mL and FGF19 to 76.17±22.79 pg/mL in the complicated group (P<0.001).

Differences in expression of inflammation- and tissue remodelling-related markers

Biliary obstruction accompanied by epithelial injury can trigger both local and systemic inflammatory responses, and this was one of the clearest features distinguishing complicated GS from simple disease. The present results showed that patients in the complicated group exhibited marked systemic inflammatory activation, along with abnormal tissue remodelling. Among routine inflammatory markers, the acute-phase proteins CRP and PCT were elevated in the complicated group (P<0.001), and the

Table IV Comparison of inflammation- and tissue remodelling-related markers between the simple GS and complicated GS groups.

Indicators	unit	Simple group (n=49)	Complicated group (n=58)	t	P
CRP	mg/L	4.59±2.22	15.34±7.32	9.90	<0.001
PCT	ng/mL	0.27±0.04	0.58±0.12	16.61	<0.001
IL-6	pg/mL	13.05±1.03	28.59±5.50	19.47	<0.001
TNF-α	pg/mL	12.25±3.10	19.81±6.15	7.80	<0.001
NLR	-	4.48±0.88	6.46±2.62	5.05	<0.001
PLR	-	120.02±27.13	157.21±57.51	4.15	<0.001
MPO	ng/mL	54.32±18.22	78.84±39.76	3.98	<0.001
Presepsin	pg/mL	70.74±26.84	205.24±52.37	16.26	<0.001
MMP-9	ng/mL	86.82±27.16	225.83±50.83	17.18	<0.001
TIMP-1	ng/mL	92.69±33.97	209.21±75.99	9.92	<0.001

Note: C-reactive protein (CRP), procalcitonin (PCT), interleukin-6 (IL-6), tumour necrosis factor-a (TNF-α), Neutrophil/lymphocyte ratio (NLR), platelet/lymphocyte ratio (PLR), Myeloperoxidase (MPO), matrix metalloproteinase-9 (MMP-9), and tissue inhibitor of metalloproteinase-1 (TIMP-1)

Table V Comparison of electrolyte and acid-base homeostasis indices between the simple GS and complicated GS groups.

Indicators	unit	Simple group (n=49)	Complicated group (n=58)	t	P
K^+	mmol/L	4.11±0.33	3.90±0.48	2.52	0.013
Na^+	mmol/L	140.28±2.34	138.06±3.64	3.69	<0.001
Cl^-	mmol/L	103.16±2.41	100.86±3.76	3.69	<0.001
Ca^{2+}	mmol/L	2.32±0.14	2.18±0.18	4.38	<0.001
iCa^{2+}	mmol/L	1.17±0.05	1.08±0.07	7.30	<0.001
Mg^{2+}	mmol/L	0.91±0.08	0.84±0.11	3.91	<0.001
P	mmol/L	1.17±0.24	1.03±0.26	2.94	0.004
Whole blood pH	-	7.41±0.04	7.37±0.05	5.36	<0.001
SBC	mmol/L	24.29±1.33	21.11±2.22	8.77	<0.001
BE	mmol/L	0.27±1.04	-3.36±1.81	12.43	<0.001

Note: serum potassium (K^+), sodium (Na^+), chloride (Cl^-), total calcium (Ca^{2+}), ionized calcium (iCa^{2+}), magnesium (Mg^{2+}), and phosphorus (P), Standard Bicarbonate (SBC), Base Excess (BE)

Table VI Comparison of bile acid subspecies profiles between the simple GS and complicated GS groups.

Indicators		Unit	Simple group (n=49)	Complicated group (n=58)	t	P
Unconjugated bile acids	CA	μmol/L	0.22±0.07	1.36±0.59	13.47	<0.001
	CDCA	μmol/L	0.36±0.11	1.97±0.84	12.73	<0.001
	DCA	μmol/L	0.43±0.13	1.25±0.55	15.18	<0.001
	LCA	μmol/L	0.05±0.02	0.19±0.08	4.40	<0.001
	UDCA	μmol/L	0.13±0.04	0.38±0.18	6.37	<0.001
Conjugated bile acid	GCA	μmol/L	0.60±0.18	6.10±2.68	15.09	<0.001
	TCA	μmol/L	0.32±0.11	3.46±1.68	10.75	<0.001
	GCDCA	μmol/L	0.87±0.24	7.81±3.30	15.63	<0.001
	TCDCA	μmol/L	0.43±0.14	4.41±2.09	12.54	<0.001
	GDCA	μmol/L	0.65±0.19	3.96±1.75	14.73	<0.001
	TDCA	μmol/L	0.28±0.09	2.18±1.02	14.41	<0.001
	GLCA	μmol/L	0.08±0.03	0.45±0.21	13.63	<0.001
	TLCA	μmol/L	0.03±0.01	0.18±0.09	1.92	<0.001
	GUDCA	μmol/L	0.15±0.05	0.72±0.32	2.05	0.043
	TUDCA	μmol/L	0.07±0.03	0.34±0.17	10.81	<0.001

Note: Cholic acid (CA), Chenodeoxycholic acid (CDCA), Deoxycholic acid (DCA), Lithocholic acid (LCA), Ursodeoxycholic acid (UDCA), Glycocholic acid (GCA), Taurocholic acid (TCA), Glycochenodeoxycholic acid (GCDCA), Taurochenodeoxycholic acid (TCDCA), Glycodeoxycholic acid (GDCA), Taurodeoxycholic acid (TDCA), Glycolithocholic acid (GLCA), Taurolithocholic acid (TLCA), Glycoursodeoxycholic acid (GUDCA), Tauro Ursodeoxycholic acid (TUDCA)

pro-inflammatory cytokines IL-6 and TNF-α were also increased (P<0.001). Of note, Presepsin, an early marker of monocyte/macrophage activation, and MPO, a marker of neutrophil activation, were both higher in the complicated group (P<0.001). MMP-9 and TIMP-1, both involved in biliary tissue injury and remodelling, were likewise several times higher in the complicated group (P<0.001).

Differences in expression of electrolyte, acid-base homeostasis, and derived indicators

Compared with the simple group, patients in the complicated group showed clear disturbance of the internal milieu. Among the core electrolyte indices, electrolyte levels in the complicated group were reduced to varying degrees (P<0.001), and the decreases in serum sodium, total calcium, and ionized calcium all exceeded 5%. Acid-base indices further suggested compensated metabolic acidosis in the complicated group, as whole-blood pH, SBC, and BE were all significantly lower than those in the simple group. The mean BE was only -3.36±1.81 mmol/L (P<0.001).

Differences in expression of the bile acid subspecies profile

Finally, absolute quantification of bile acid subspecies showed that each measured bile acid was higher in the complex group than in the simple group (P<0.001), although the magnitude of the increase varied markedly across subtypes. Conjugated bile acids rose much more sharply than unconjugated species: glycine- and taurine-conjugated bile acids were on average 8–10 times higher, whereas unconjugated bile acids increased by only 2- to 5-fold. Among the unconjugated bile acids, CDCA showed the greatest increase, rising by approximately 4.5-fold. Overall, this profile closely matched the pattern expected in biliary obstruction accompanied by interruption of the enterohepatic circulation.

Discussion

This study systematically compared the preoperative peripheral blood biochemical profiles of 107 patients with simple and complicated GS to characterize changes in multipathway biochemical indices during GS progression. We ultimately identified significant between-group differences in core cholestatic markers, bile duct injury-specific indices, inflammation- and tissue remodelling-related factors, electrolyte and acid-base homeostasis, and the bile acid subspecies profile. Taken together, these findings outline the coordinated multidimensional biochemical changes that accompany the shift from simple to complicated disease.

These characteristic differences were initially reflected in the cholestasis-related indicators. Patients with complicated GS exhibited a bilirubin profile typical of biliary obstruction, with marked increases in total and direct bilirubin, accompanied by several-fold elevations in bile duct-associated enzymes such as GGT and ALP. In essence, this is the direct biochemical expression of an interrupted bile excretory pathway after biliary obstruction (9). Once biliary excretion is impaired, conjugated bilirubin actively secreted by hepatocytes can no longer enter the intestine and instead refluxes directly into the systemic circulation. Meanwhile, membrane-bound enzymes from biliary epithelial cells are released into the bloodstream in large amounts as epithelial barrier injury worsens and membrane permeability increases, making them sensitive biochemical indicators of the degree of obstruction (10, 11).

In the present study, GST-α, a bile duct epithelial injury-specific marker, was also elevated in patients with complicated GS, whereas FGF19 and C4, two key indices of the bile acid metabolic regulatory axis, were both reduced. As an enzyme specifically expressed in the cytoplasm of biliary epithelial cells, GST-α is released into the circulation in substantial amounts only when the epithelial barrier is damaged. Its specificity for detecting biliary epithelial injury is therefore much higher than that of conventional transaminases derived from hepatocytes (12). This pattern also aligns with earlier biochemical observations in benign biliary obstruction (13). The parallel decline in FGF19 and C4 appears to stem chiefly from interruption of the enterohepatic circulation of bile acids. When biliary obstruction occurs, bile acids in the intestinal lumen become depleted, and synthesis and secretion of FGF19 by the ileal epithelium drop accordingly. At the same time, intrahepatic retention of bile acids activates the farnesoid X receptor, strongly suppressing the rate-limiting enzyme CYP7A1 in bile acid synthesis. C4 is a direct downstream product of CYP7A1-mediated cholesterol hydroxylation. It thus serves as a reliable indirect marker of hepatic bile acid synthesis rate, which ultimately leads to a reduction in circulating C4 levels (14–16).

Biliary obstruction does more than mechanically interrupt bile flow; through the cytotoxic effects of retained bile acids, it can also sustain an inflammatory cascade (17). This was well reflected in the inflammatory marker profile observed here. In patients with complicated GS, acute-phase proteins and pro-inflammatory cytokines were both elevated. At the same time, MPO, a neutrophil activation marker, and Presepsin, an early marker of monocyte/macrophage activation, also increased in parallel. Together, these findings point to broad activation of innate immune cells under obstructive conditions. Retained hydrophobic bile acids can directly damage biliary epithelial cell membranes and induce the release of damage-associated molecular patterns, which then recruit and activate neutrophils and monocyte/macrophages. The result is the release of large amounts of pro-inflammatory mediators and the establishment of a vicious cycle linking cholestasis, epithelial injury, and inflammatory activation (18, 19). In our view, this is the central mechanism behind the synchronous rise in multiple inflammatory markers seen in this study. We also observed concurrent upregulation of MMP-9 and TIMP-1, reflecting an inflammation-driven remodelling process in biliary tissue. Activated macrophages can secrete large amounts of MMP-9 to degrade the extracellular matrix and participate in tissue repair at injury sites, whereas the simultaneous increase in the endogenous inhibitor TIMP-1 likely represents a compensatory response aimed at limiting excessive matrix degradation. This dynamic pattern is consistent with previous biochemical findings related to tissue injury and repair (20, 21).

Persistent inflammatory activation together with cholestasis can further destabilize internal homeostasis (22). In the present study, patients with complicated GS displayed clear electrolyte disturbances and compensated metabolic acidosis. Under inflammatory conditions, increased vascular permeability may lead to extravascular loss of electrolytes, while tissue hypoxia induced by infectious stress promotes lactate production and thereby contributes to metabolic acidosis with an increased anion gap. To compensate for acidosis, the body increases renal potassium excretion, ultimately giving rise to statistically significant reductions in serum potassium and sodium levels, with a proportion of patients progressing to clinically evident hypokalaemia and hyponatremia. This is a classic biochemical pattern of disturbance in the internal milieu under infectious stress (23). It is worth noting that the increase in conjugated bile acids observed in this study was much greater than that in unconjugated bile acids, and the rise in primary

bile acids was clearly greater than that in secondary bile acids. This pattern differs substantially from the bile acid spectrum typically seen in cirrhosis. As is well known, the core pathological change in cirrhosis is impairment of hepatocellular synthetic function, together with reduced bile acid conjugation capacity (24); accordingly, the increase in serum bile acids is mainly driven by unconjugated bile acids.

In contrast, the patients with GS included in this study had preserved hepatocellular synthetic and conjugative function, with the main defect lying in biliary excretion. A reasonable explanation is that conjugated bile acids actively secreted by hepatocytes were unable to enter the intestine and instead refluxed directly into the systemic circulation, becoming the principal contributor to the increase in serum bile acids. At the same time, depletion of intestinal bile acids may have reduced the substrate available for secondary bile acid formation, ultimately leading to the characteristic bile acid profile observed here.

However, as a single-centre, retrospective observational study, the present work had a limited sample size and may therefore be subject to some selection bias. Further validation in multicentre studies with larger cohorts is still needed. In addition, because no perioperative dynamic monitoring was performed, we are currently unable to define how these biochemical markers change over time as the disease progresses, nor can we clearly establish the temporal relationship between marker variation and disease progression. Additionally, no multivariate Logistic regression analysis was performed to identify independent risk factors for complicated GS, thereby limiting the clinical predictive value of the identified biochemical markers. Finally, this study focused only on differences in expression and correlation among clinical biochemical indices. No cell-based or animal experiments were carried out to verify the underlying molecular regulatory mechanisms, and the causal role of these markers in GS progression therefore remains uncertain. These issues merit further investigation in future basic studies.

Conclusion

Through a systematic analysis of multi-dimensional biochemical indices, this study clarified differences in the preoperative biochemical profile between patients with simple and complicated GS and revealed that cholestasis, inflammatory activation, disturbance of internal homeostasis, and abnormal bile acid metabolism co-evolve during disease progression. These findings provide broader laboratory biochemical evidence for understanding the pathophysiology of GS progression and also offer a data foundation and new directions for subsequent research in GS-related medical biochemistry.

Ethical approval

The study involving human subjects complied with the Declaration of Helsinki. It was approved by the ethical committee of The First People's Hospital of Chuzhou Affiliated to Anhui Medical University (Approval Number:2026LunShen-Biology-035), and all participants provided written informed consent.

Acknowledgements. Not applicable.

Funding

Not applicable.

Availability of data and materials

The datasets generated during and/or analysed during the current study are available from the corresponding author on reasonable request.

Authors' contribution

Xuecui Ge and Tingting Zhang contributed equally to this work.

Conflict of interest statement

All the authors declare that they have no conflict of interest in this work.

References

1. Verdonk RC, de Zeeuw S, de Reuver PR. [Gallstones]. Ned Tijdschr Geneeskd 2024; 168.
2. Wu W, Pei Y, Wang J, Liang Q, Chen W. Association of dietary quality indicators with gallstones in the US: NHANES 2017-2020. BMC Public Health 2025; 25(1): 976.
3. Phillpotts S, Webster G, Arvanitakis M. Endoscopic Management of Complex Biliary Stones. Gastrointestinal endoscopy clinics of North America 2022; 32(3): 477–92.
4. Podboy A, Gaddam S, Park K, Gupta K, Liu Q, Lo SK. Management of Difficult Choledocholithiasis.

Digestive diseases and sciences 2022; 67(5): 1613–23.

5. Jalan-Sakrikar N, Guicciardi ME, O'Hara SP, Azad A, LaRusso NF, Gores GJ, et al. Central role for cholangiocyte pathobiology in cholestatic liver diseases. Hepatology 2025; 82(4): 834–54.
6. Jones MW, Weir CB, Marietta M. Gallstones (Cholelithiasis). StatPearls. Treasure Island (FL) ineligible companies. Disclosure: Connor Weir declares no relevant financial relationships with ineligible companies. Disclosure: Mia Marietta declares no relevant financial relationships with ineligible companies: StatPearls Publishing Copyright © 2026, StatPearls Publishing LLC.; 2026.
7. Bai Y, Zhang M, Chen L, Zhou P, Zhou B, Wang R, et al. Gastrointestinal traits, common inflammatory disorders, gallstones, and biliary tract cancer: A network Mendelian randomization study. J Adv Res 2026; 79: 15–22.
8. Volkovetskii V, Lobanova O, Puzyr N, Tkachenko A, Maksimenko M, Rudyk M, et al. Laparoscopic common bile duct exploration vs endoscopic retrograde cholangiopancreatography for the treatment of difficult common bile duct stones: postsurgery inflammation and liver function. Journal of gastrointestinal surgery: official journal of the Society for Surgery of the Alimentary Tract 2025; 29(9): 102156.
9. Zhang X, Guan L, Tian H, Li Y. Prevalence and Risk Factors of Gallbladder Stones and Polyps in Liaoning, China. Front Med (Lausanne) 2022; 9: 865458.
10. Sun H, Warren J, Yip J, Ji Y, Hao S, Han W, et al. Factors Influencing Gallstone Formation: A Review of the Literature. Biomolecules 2022; 12(4).
11. Lammert F, Wittenburg H. Gallstones: Prevention, Diagnosis, and Treatment. Semin Liver Dis 2024; 44(3): 394–404.
12. Tamber SS, Bansal P, Sharma S, Singh RB, Sharma R. Biomarkers of liver diseases. Mol Biol Rep 2023; 50(9): 7815–23.
13. Tamme K, Acosta S, Biloslavo A, Björck M, Casian D, Damaskos D, et al. Biomarkers in Prediction of Acute Mesenteric Ischemia: a prospective multicentre study (BIPAMI study): a study protocol. BMC Surg 2024; 24(1): 201.
14. Mohammed TA, Zalzala MH. Farnesoid X Receptor-Mediated Bile Acids Regulation in Cholestasis. Indian Journal of Clinical Biochemistry 2026; 41(2): 181–7.
15. Li C, Chen T, Liu J, Wang Y, Zhang C, Guo L, et al. FGF19-Induced Inflammatory CAF Promoted Neutrophil Extracellular Trap Formation in the Liver Metastasis of Colorectal Cancer. Advanced science (Weinheim, Baden-Wurttemberg, Germany) 2023; 10(24): e2302613.
16. Li X, Lu W, Kharitonenkov A, Luo Y. Targeting the FGF19-FGFR4 pathway for cholestatic, metabolic, and cancerous diseases. Journal of internal medicine 2024; 295(3): 292–312.
17. Zhuang Y, Ortega-Ribera M, Thevkar Nagesh P, Joshi R, Huang H, Wang Y, et al. Bile acid-induced IRF3 phosphorylation mediates cell death, inflammatory responses, and fibrosis in cholestasis-induced liver and kidney injury via regulation of ZBP1. Hepatology. 2024; 79(4): 752–67.
18. Yan M, Hou L, Cai Y, Wang H, Ma Y, Geng Q, et al. Effects of Intestinal FXR-Related Molecules on Intestinal Mucosal Barriers in Biliary Tract Obstruction. Front Pharmacol 2022; 13: 906452.
19. O'Leary CE, Sbierski-Kind J, Kotas ME, Wagner JC, Liang HE, Schroeder AW, et al. Bile acid-sensitive tuft cells regulate biliary neutrophil influx. Science immunology 2022; 7(69): eabj1080.
20. Zhang WQ, Tang W, Hu SQ, Fu XL, Wu H, Shen WQ, et al. Effect of matrix metalloproteinases on the healing of diabetic foot ulcer: A systematic review. J Tissue Viability 2023; 32(1): 51–8.
21. Schoeps B, Frädrich J, Krüger A. Cut loose TIMP-1: an emerging cytokine in inflammation. Trends in cell biology 2023; 33(5): 413–26.
22. Ciesielski W, Durko Ł, Stefańczyk L, Dobek A, Bulicz A, Wojnicka A, et al. Endoscopic Ultrasound-Guided Versus Percutaneous Transhepatic Biliary Drainage After Failed Endoscopic Retrograde Cholangiopancreatography in Malignant Biliary Obstruction: A Single-Center Retrospective Cohort. Cancers (Basel) 2026; 18(5).
23. Yang X, Ou Y, Yang Y, Wang L, Zhang Y, Zhao F, et al. Targeting endothelial coagulation signaling ameliorates liver obstructive cholestasis and dysfunctional angiogenesis. Exp Biol Med (Maywood) 2023; 248(14): 1242–53.
24. Rimal B, Collins SL, Tanes CE, Rocha ER, Granda MA, Solanki S, et al. Bile salt hydrolase catalyses formation of amine-conjugated bile acids. Nature 2024; 626(8000): 859–63.

Received: April 14, 2026
Accepted: May 05, 2026